Proc. Natl. Acad. Sci. USA
Vol. 76, No. 3, pp. 1054–1058, March 1979
Biochemistry

Localization of the decoding region on the 30S *Escherichia coli* ribosomal subunit by affinity immunoelectron microscopy

(P site crosslinking of tRNA/ribosome topography/2,4-dinitrophenyl-aminobutyrylvalyl-tRNA)

MORDECHAI KEREN-ZUR, MILOSLAV BOUBLIK, AND JAMES OFENGAND

Roche Institute of Molecular Biology, Nutley, New Jersey 07110

Communicated by Severo Ochoa, November 27, 1978

ABSTRACT **The decoding region of the *Escherichia coli* ribosome has been localized by affinity immunoelectron microscopy. Valyl-tRNA$_1^{Val}$, derivatized at the α-amino end with the dinitrophenyl group, was bound to the ribosomal P site of 70S ribosomes and crosslinked specifically to 16S RNA by 310- to 325-nm irradiation. Previous work has shown that the crosslink occurs between the 5′ anticodon base of the tRNA and a pyrimidine in the 3′ one-third of the 16S RNA. By reaction of the dinitrophenyl group with antibody, dimers of the 30S tRNA covalent complexes were prepared containing one covalently attached tRNA per 30S subunit. Electron microscopic visualization of the antibody attached to the dinitrophenyl group located the position of the 3′ end of the tRNA. Several sites, with a strong preference for the large protrusion or cleft region in the upper one-third of the subunit, were found. The multiplicity of sites is likely due to the freedom of orientation of the 3′ end of the tRNA which is approximately 80 Å from the site of crosslinking. By extrapolating this distance from each of the antigenic sites, we concluded that the anticodon of tRNA when in the P site is probably located in the cleft region of the 30S subunit.**

Numerous approaches have been used to localize the A and P binding sites for tRNA on the ribosome (reviewed in ref. 1). The earlier studies (reviewed in refs. 2 and 3; see also refs. 4–7) used various procedures in the presence or absence of tRNA to modify the ribosome, but, in general, these methods were not able to distinguish between a direct action of the reagent on the binding site and an indirect effect due to a modification elsewhere. They have now largely been supplanted by the technique of affinity labeling which allows a direct determination of the close contacts between tRNA and the ribosomal surface. Affinity labeling of the ribosome from defined sites on the tRNA has been confined to the 3′ terminus (reviewed in refs. 1 and 8–10), except for our own work in which probes attached to other parts of the tRNA (11–16) were used. The former studies have resulted in the identification of proteins and RNA near to the peptidyl transferase center (reviewed in refs. 1, 8, and 10), and localization of the proteins by immunoelectron microscopy (immuno-EM) has allowed construction of a topographical map of this region on the 50S subunit (1, 8). Up to now, a similar identification of other parts of the A and P binding sites for tRNA has not been reported.

We recently observed that *Escherichia coli* AcVal-tRNA$_1^{Val}$ (and certain other tRNAs) bound at the P site of 70S ribosomes could be covalently crosslinked with high efficiency to 16S ribosomal RNA by irradiation at 310–325 nm (13). This reaction linked the anticodon loop of the tRNA to the 3′ one-third of the 16S ribosomal RNA (15, 16). Since the tRNA was covalently attached via its anticodon to the presumptive decoding region of the ribosome, the possibility of visualization of this site by EM was considered. Preliminary experiments showed that it was not possible to directly visualize tRNA on the ribosome with the present EM methods. We decided, therefore, to attach a suitable antigenic determinant to the tRNA in order to use antibody (Ab) against it as a marker for the location of the tRNA molecule. This technique, which we call affinity immuno-EM, has provided a direct approach to localization of the decoding region on the 30S particle.

MATERIALS AND METHODS

***N*-(γ-Dinitrophenyl)aminobutyryl (DNP-Abu)[^{3}H]Val-tRNA.** DNP-Abu (Sigma) was coupled to *N*-hydroxysuccinimide (HONSu) with *N*,*N*′-dicyclohexylcarbodiimide in dimethylformamide. Esterification was followed by silica gel thin-layer chromatography (Eastman) developed with ethyl acetate/methanol (10:1). The R_F of DNP-Abu = 0.1; R_F of DNP-Abu-ONSu = 0.9. After isolation, the product was tested by reaction with glucosamine. There was complete conversion to a new product, possessing an R_F of 0.48 (the R_F of DNP-Abu was 0.86 and the R_F of DNP-Abu-ONSu was 0.9) when analyzed by silica gel thin-layer chromatography developed with chloroform/methanol/HOAc (65:30:5). DNP-Abu-ONSu, 14 mM, was reacted with 11 μM [^{3}H]Val-tRNA/50 mM triethanolamine·HCl, pH 8.7/70% aqueous *N*,*N*-dimethylformamide at 23°C. The extent of acylation was monitored by Cu^{2+}–Tris catalyzed hydrolysis (13, 17). The $t_{1/2}$ for the reaction was about 25 min. The reaction was stopped after 2 hr (95% acylation) by precipitation with 0.1 vol of 20% KOAc, pH 5, and 0.5 vol of EtOH. Less than 2% of the radioactivity was found in the supernatant. The tRNA was further purified over Sephadex G-50 in 10% aqueous EtOH. About 87% of the radioactivity was found in the tRNA fraction.

Other Materials. [^{3}H]Valine (11.5 Ci/mmol, 1 Ci = 3.7 × 10^{10} becquerels) and ε-[^{3}H]DNP-Lys (4.9 Ci/mmol) were from New England Nuclear. [^{3}H]Val-tRNA and Ac[^{3}H]Val-tRNA were prepared as described (13). Poly(U_2,G) and tRNA^{Val} were purchased from Boehringer Mannheim. Tight couple ribosomes were prepared according to the procedures described by Noll *et al.* (18). High affinity rabbit anti-DNP IgG was obtained from Gateway Immunosera Co. (P. O. Box 1735, Cahokia, IL 62206).

Ribosomal P Site Binding. The reaction was carried out and assayed as described (15) except that the poly(U_2,G) concentration was 40 μg/ml, the ribosome concentration was 212 nM, the acylaminoacyl-tRNA concentration was as specified, and incubation was for 10 min at 37°C.

Irradiation. tRNA–ribosome mixtures were irradiated at 0°C with 300-nm light in a Rayonet RPR photoreactor (fig. 5 in ref. 13; ref. 15) modified to include a 1-cm-path solution filter consisting of 1.7 M $NiSO_4$ to protect the DNP group (λ_{max} of 360 nm) against possible photoreaction. The Mylar filter was removed in order to shorten the irradiation period (15) and so

The publication costs of this article were defrayed in part by page charge payment. This article must therefore be hereby marked "*advertisement*" in accordance with 18 U. S. C. §1734 solely to indicate this fact.

Abbreviations: DNP-, 2,4-dinitrophenyl; HONSu, *N*-hydroxysuccinimide; DNP-Abu, *N*-(γ-dinitrophenyl)aminobutyric acid; Ab, antibody; EM, electron microscopy.

lessen the exposure of the DNP group. In a control experiment, irradiation of [^{3}H]DNP-Lys for 100 min did not affect (<5%) its binding to anti-DNP.

Sucrose Gradient Centrifugation. DNP-Abu[^{3}H]Val-tRNA–30S covalent complexes were separated from 50S and noncovalently bound tRNA by centrifugation at 39,000 rpm for 6 hr at 3°C in an SW-40 rotor through a 10–30% sucrose gradient in buffer A [10 mM Hepes (pH 7.5), 100 mM NH_4Cl, 1.1 mM $Mg(OAc)_2$, 0.1 mM EDTA]. To remove contaminants, the sucrose was filtered through a Nalgene 0.2-μm membrane (cat. no. 120), ultrafiltered through an Amicon UM-2 membrane, and again passed through a fresh Nalgene 0.2-μm membrane. Where indicated, the pooled 30S fractions were concentrated, and the sucrose was removed with a Millipore molecular separator apparatus (80–100% recovery).

Immunological Reactions. (*i*) Binding of DNP-Abu[^{3}H]-Val-tRNA or [^{3}H]DNP-Lys to Ab was carried out by incubation of the DNP-containing compound (0.1–10 nM) with anti-DNP in Ab reaction buffer (10 mM potassium phosphate, pH 6.5/0.1 M NaCl) for 2 min at 37°C followed by 20 min at 0°C. The mixtures were diluted to 1 ml with Ab reaction buffer, filtered through a Gelman GN-6 membrane filter (19, 20), rinsed with cold Ab reaction buffer (2 × 2 ml), and assayed for radioactivity. With excess anti-DNP, the amount of [^{3}H]DNP-Lys or DNP-Abu[^{3}H]Val-tRNA bound was proportional to the amount added. With limiting anti-DNP, bound DNP was proportional to the amount of Ab added. By either assay, the binding efficiency was 60–70%. This assay was not suitable for ribosome-bound antigens, because ribosomes are also retained by the membrane filter.

(*ii*) The anti-DNP titer was determined with the filter binding assay by adding increasing amounts of anti-DNP to 1 pmol of [^{3}H]DNP-Lys. The minimal quantity of anti-DNP needed to reach a plateau value of [^{3}H]DNP-Lys bound to the filter was taken to be equivalent to the amount of DNP-Lys added.

(*iii*) Dimers of DNP-Abu-Val-tRNA–30S ribosomal covalent complexes were obtained by the addition of anti-DNP to ribosomes in buffer A at 37°C. In order to maximize the yield of dimers, ribosome excess was maintained by adding the antibody in portions at 5 min intervals. The last portion was added at 0°C to minimize conversion of dimers into monomers. The reaction mixture was incubated for an additional 30 min at 0°C before application to the sucrose gradient.

EM. Specimens for EM were prepared as described (21). Adsorption of the Ab–DNP-Abu-Val-tRNA–30S complexes (in buffer A) to the carbon support was done in parallel at room temperature and at 4°C at intervals after isolation from the sucrose gradient. A 0.5% aqueous uranyl acetate solution was used as a contrasting solution. The grids were examined in a JEM 100B electron microscope operated at 80 kV and a direct magnification of 70,000. Printing was done with the plate emulsion facing the paper emulsion. Ribosomal particles were scanned on photographic enlargements of EM images for statistical evaluation of the attachment site of the antibody to the DNP-Abu-Val-tRNA–30S covalent complexes.

RESULTS

Hapten Labeling of the tRNA. The amino acid end of Val-tRNA was chosen as the labeling target because (*i*) *N*-blocked amino acyl-tRNAs bind to the P site where $tRNA_1^{Val}$ can be crosslinked to the ribosome (13, 15), (*ii*) *N*-acylation of the amino acid proceeds under mild conditions with high yield and specificity, and most importantly (*iii*) the amino acid end of the tRNA was expected to be the most highly exposed for interaction with Ab. More than 95% of the Val-tRNA amino groups were blocked. In a control experiment, uncharged tRNA was mixed with the reagent and purified under exactly the same conditions. The amount of DNP groups introduced into the deacylated tRNA was determined by radioimmunoassay. The test system, [^{3}H]DNP-Lys and anti-DNP, was calibrated with DNP-Abu-Val-tRNA. Less than 40 pmol of DNP per A_{260} unit of uncharged tRNA was found, indicating that more than 97% of the DNP bound to Val-tRNA was attached to the amino acyl residue, assuming a theoretical value of 1.5 nmol/A_{260} unit. DNP-Abu[^{3}H]Val-tRNA readily formed a complex with anti-DNP, which could be detected by the filter binding assay (data not shown).

DNP-Abu-Val-tRNA could be bound to the ribosomal P site as well as control AcVal-tRNA. About 75% of the DNP-Abu-Val-tRNA added could be bound with excess ribosomes, compared to 70% for AcVal-tRNA. Omission of poly(U_2,G) reduced the binding to 1/10th to 1/30th of the original value, indicating the specificity of the binding, and, as shown previously for AcVal-tRNA (13), this binding was exclusively to the ribosomal P site, because 92% of the noncovalently bound DNP-Abu[^{3}H]Val-tRNA could be released by puromycin treatment (data not shown due to space limitations).

Covalent Attachment of DNP-Abu-Val-tRNA to the Ribosomes. Irradiation of DNP-Abu-Val-tRNA–ribosome noncovalent complexes gave increasing amounts of crosslinked product until a plateau was reached at about 100 min. The degree of crosslinking achieved after 125 min was determined by sucrose gradient analysis at 1 mM Mg^{2+} of ribosomes photoreacted in the presence of either DNP-Abu-Val-tRNA or AcVal-tRNA (Fig. 1). At this Mg^{2+} concentration, ribosomes dissociate into subunits and release tRNA that is not covalently bound. Both DNP-Abu-Val-tRNA and AcVal-tRNA crosslinked exclusively to the 30S subunits. No 50S attachment was detected, which would have been expected for a 3′-end affinity label (8) if any crosslinking had occurred via the DNP group. Of the noncovalently bound DNP-Abu-Val-tRNA and AcVal-tRNA, 45 and 36%, respectively, became attached, and all of the crosslinking was poly(U_2,G) dependent. The crosslinked tRNA was located in the P site, because, after irradiation, more than 90% of the ribosome-associated Ac[^{3}H]Val could be released by puromycin treatment (data not shown). The same result was found for the crosslinking of AcVal-tRNA (13, 15).

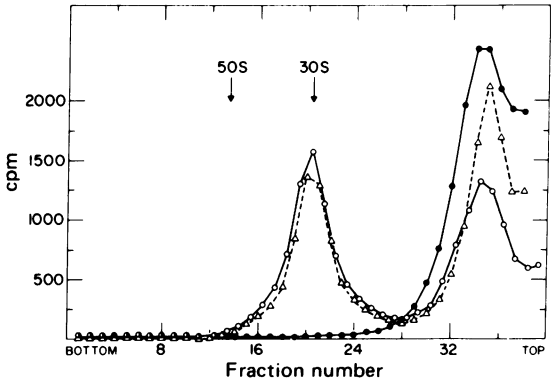

FIG. 1. Crosslinking of DNP-Abu[^{3}H]Val-tRNA to 30S ribosomal subunits. Ribosomal P site binding mixtures, containing either 138 nM Ac[^{3}H]Val-tRNA (△), or 125 nM DNP-Abu[^{3}H]Val-tRNA in the absence (●) or in the presence (○) of poly(U_2,G) (59, 4, and 69% of these tRNAs were noncovalently bound, respectively) were irradiated for 125 min. The amount of crosslinking, determined by the filter assay (13), was 30, 3, and 35% of the bound tRNA, respectively. After poly(U_2,G) addition to the second reaction mixture (●) and 10 min of incubation at 37°C, the noncovalent binding of DNP-Abu[^{3}H]-Val-tRNA increased from 4 to 55%. The three reaction mixtures were analyzed by sucrose gradient centrifugation. Aliquots (30 μl) from the fractions (330 μl) were counted. Of the recovered radioactivity, 36, 1, and 45%, respectively, was associated with the 30S peak.

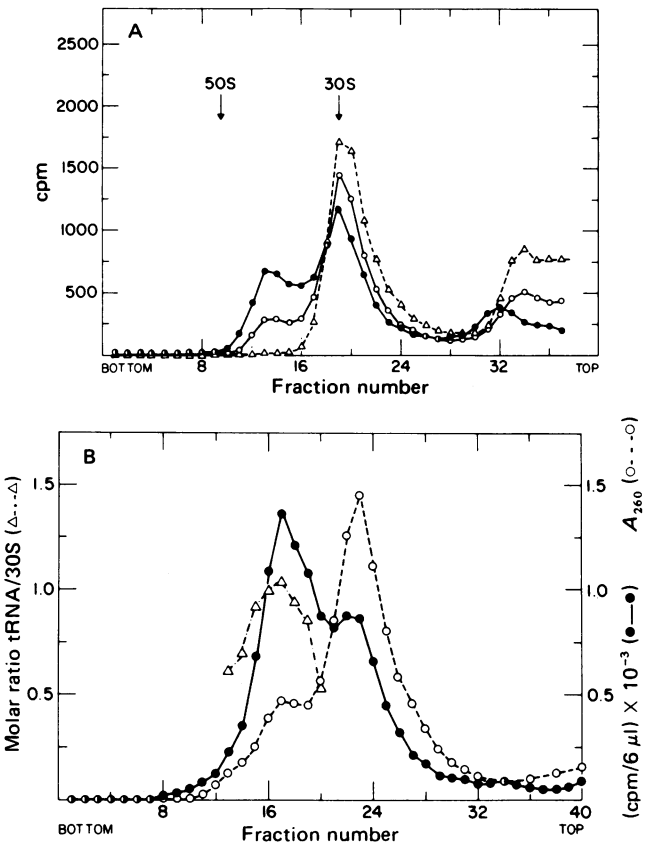

FIG. 2. Dimerization of DNP-labeled 30S ribosomal subunits with anti-DNP. (*A*) DNP-Abu-Val-tRNA–30S complexes, 2.8 pmol, prepared as in Fig. 1, were added in buffer A to anti-DNP, 0.4 equivalents (○), 0.8 equivalents (●), or 0.8 equivalents plus 200 pmol of DNP-Abu (△). The Ab was added in three equal portions to a final volume of 0.12 ml. Samples were analyzed by sucrose gradient centrifugation. About 12, 27, and <1%, respectively, of the ribosome-associated radioactivity was found in the dimer region. (*B*) P site complexes (6 ml) with 125 nM DNP-Abu[^{3}H]Val-tRNA (68% of the tRNA was noncovalently bound) were irradiated for 190 min, concentrated 6-fold, and purified by two successive sucrose gradient centrifugations. To the purified 30S subunits containing 140 pmol of crosslinked DNP-Abu[^{3}H]Val-tRNA (0.38 mol of tRNA per mole of 30S) in a final volume of 0.3 ml was added 0.9 equivalent of anti-DNP in four equal portions. The Ab complexes were separated by sucrose gradient centrifugation. The molar ratio of tRNA to 30S subunits was calculated from the cpm/A_{260} unit assuming that 1 pmol of 30S is 0.015 A_{260} unit and 1 pmol of [^{3}H]Val-tRNA corresponds to 6965 cpm.

Interaction of DNP-Abu-Val-tRNA–30S Complexes with Anti-DNP. The addition of divalent Ab to ribosomes containing a single DNP group can lead only to dimer formation. 30S dimers have a higher S value than the monomer and can be separated from the monomer by sucrose gradient centrifugation (20, 22, 23). Fig. 2*A* shows a sucrose gradient analysis at 1 mM Mg^{2+} of such reaction mixtures. Upon addition of Ab to the DNP-Abu[^{3}H]-Val-tRNA–30S complex (DNP-labeled 30S ribosomes), a new faster sedimenting radioactive peak appeared, which increased when more anti-DNP was added. Thus, 12% and 27% of the ribosome-associated radioactivity was found in the dimer peak when 0.4 and 0.8 equivalents of anti-DNP were added, respectively. However, in the presence of an excess of DNP-Abu this peak was abolished completely. This control proves that the new peak arose as a result of the availability of DNP binding sites on the Ab. In order to show that only the added DNP groups were capable of reaction with the Ab, Ac[^{3}H]Val-tRNA–30S complexes were mixed with the same amount of anti-DNP and centrifuged. No dimer peak was found, indicating that no other group on the ribosome or tRNA could form this complex with the Ab (data not shown). The S value of the dimer, calculated from Fig. 2*A*, is 42 ± 2 S, in agreement with the value that can be calculated from the data of Tischendorf *et al.* (22) and Politz and Glitz (20).

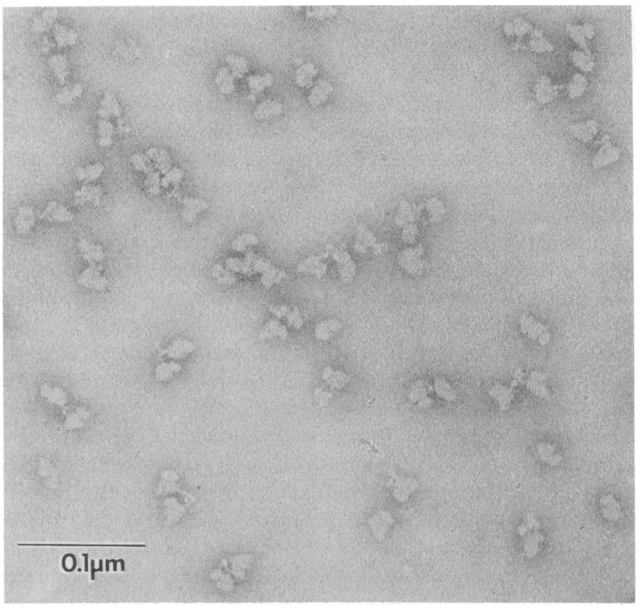

FIG. 3. Electron micrograph of a typical field of anti-DNP–30S dimers. (×167,000.)

The formation and separation of dimers from monomers was a powerful purification tool, because only those 30S subunits that carried a covalently attached DNP-Abu-Val-tRNA were capable of dimer formation. Thus, in one step inactive 30S subunits and particles that bound tRNA but failed to crosslink were removed. On a preparative scale (Fig. 2*B*), about 60% of the DNP-Abu-Val-tRNA was found in the dimer peak, in contrast to the value of 27% dimerization found in the analytical experiment (Fig. 2*A*) which was done identically except at a lower concentration of 30S (23 nM compared to 500 nM). Only 20% of the A_{260} of the 30S subunits was found in the dimer peak because only 38% of the particles were crosslinked. The molar ratio of tRNA to 30S subunits, calculated from the cpm/A_{260} units for each fraction, was essentially one.

EM. Portions of the peak fractions, 16 and 17 in Fig. 2*B*, were taken for EM examination (Fig. 3). The best results were obtained when the specimens were adsorbed to the carbon support at 4°C immediately after sucrose gradient centrifugation. Under these conditions, as much as 50% of the ribosomal particles remained in the form of dimers, 9% were found as single particles with attached Ab (monomers), and the rest were free 30S particles. Adsorption at room temperature lowered the yield of dimers by only 5%, and the effect of a 1:10 dilution with buffer A (necessary for lowering the sucrose concentration) was insignificant. However, a dramatic decrease in the amount of dimers, to 25%, was observed when the specimen was adsorbed to the support grid after a 24-hr storage at 4°C. The amount of monomers (10%) was unchanged.

Electron micrographs of monomers with interpretive drawings are shown in Fig. 4*A*. The Y-shaped Ab serves as a marker solely for the site of the amino acid end of the tRNA molecule because, as indicated above, more than 97% of the bound DNP was at the amino acid position. The gallery represents approximately the observed distribution of sites. Fig. 4*B* shows a gallery of dimers selected to show various positions. The antibody makes a distinct visible junction between the two 30S subunits.

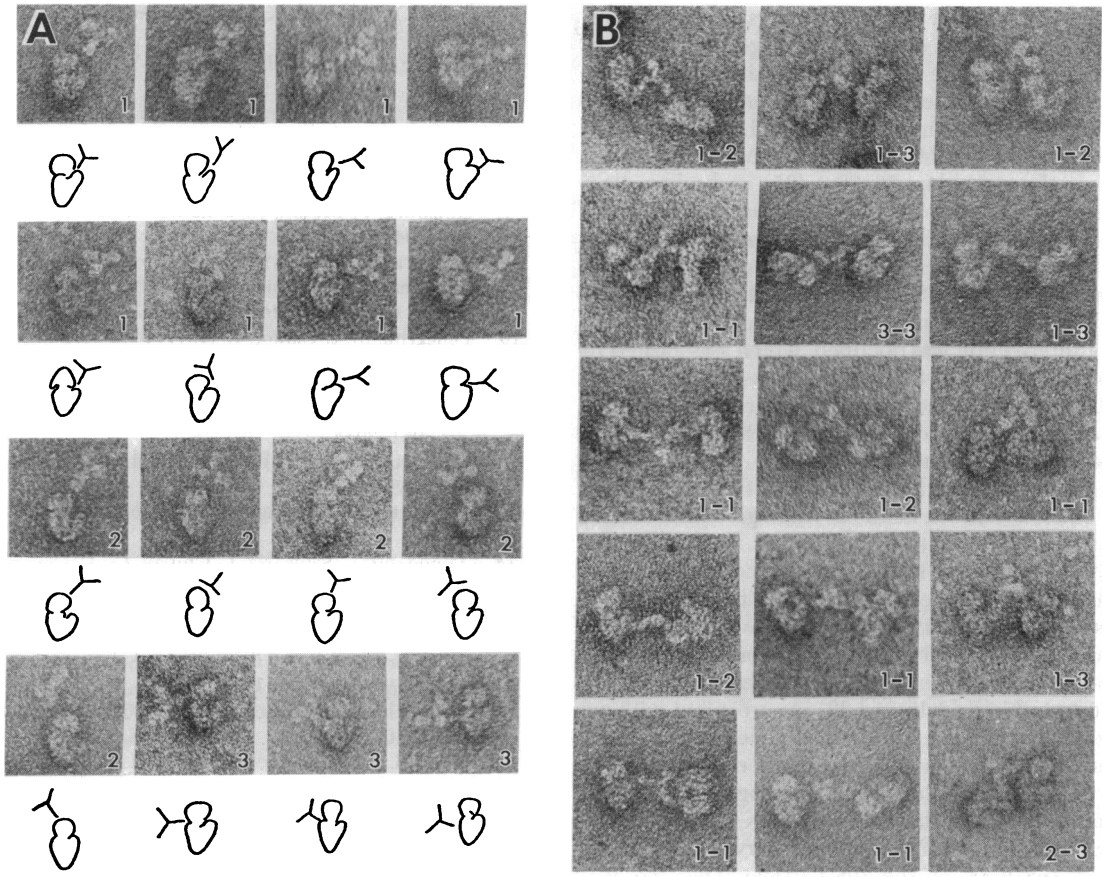

FIG. 4. Electron micrographs of anti-DNP–30S subunit complexes. (*A*) Monomers with interpretive drawings. (*B*) Dimers of 30S subunits with attached anti-DNP. The numbers on each electron micrograph identify the sites of Ab attachment as defined in Fig. 5. (×390,000.)

The location of the various binding sites is shown in Fig. 5 which also illustrates the shape of the 30S subunit as visualized by our technique. The distribution of Ab among these binding sites is given in Table 1. More than 50% of the monomers and almost 70% of the dimers had Ab attached to position 1, covering the right-hand side projection and the cleft. The frequency of attachment to areas 2 and 3 was much lower, about 15–20%. There was virtually no attachment to areas 4 and 5.

DISCUSSION

The DNP-Abu-Val-tRNA used in these experiments was functionally active. Ribosomal binding as well as crosslinking was dependent on mRNA (Fig. 1), and reaction with puromycin showed that all of the tRNA remained in the P site even after the crosslinking reaction was completed. One of the reasons for preferring affinity labeling over generalized RNA/protein or RNA/RNA crosslinking is the possibility to carry out such functional tests after covalent linking has occurred. The DNP group was present only at the 3′ end of the Val-tRNA, and the formation of 30S dimers was completely dependent on the presence of these DNP groups as well as on Ab with functionally active binding sites (Fig. 2). Therefore, Ab bound to the DNP hapten served as a specific marker of the 3′ end of the tRNA.

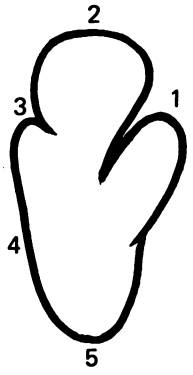

FIG. 5. Schematic drawing of the 30S *E. coli* ribosomal subunit. The attachment sites of the antibody to the subunit are denoted as 1–5. The particle dimensions are 220 × 100 Å (24).

Table 1. Distribution of sites of antibody attachment to 30S subunits

Position	Percentage In monomers	Percentage In dimers	Dimer distribution Type	Dimer distribution Percentage
1	56	66	1-1	41
			1-2	26
2	24	18	1-3	20
			1-4	3
3	16	13	2-2	3
			2-3	3
4	3	2	2-4	1
			3-3	2
5	<1	<1	4-5	<1

The location of the various positions on the 30S subunit is shown in Fig. 5. The data of column 4 were calculated by considering the distribution of positions rather than the distribution of particles. Thus a 1-1 particle is scored as two 1 positions, a 1-2 particle as one 1 plus one 2 position, etc. A total of 240 monomers and 130 dimer particles was examined.

The major resolution limit to the EM results described here is the freedom of orientation of the DNP antigen at the amino acid end of the tRNA, some 83 Å from the site of ribosomal attachment. This value, which is only an approximation, was obtained by adding the maximal distance of the DNP antigen from the 3′ hydroxyl of tRNA (about 15 Å) to the distance of the 3′ end from the anticodon, 76–83 Å (25), and subtracting 12 Å, which is the distance of the DNP binding site from the periphery of the Ab (26). This relatively long distance may explain why apparent multiple binding sites were found from a supposed single point of attachment. By extrapolating 83 Å from each of the predominant sites of attachment, an approximate area of intersection was obtained, which was located in the region of the cleft of the 30S subunit. We suggest that this is likely to be the point of covalent attachment of the tRNA anticodon to the 3′ one-third of 16S RNA and, therefore, should be the decoding region of the ribosome.

This conclusion agrees with the location of the decoding site deduced by other, less direct, methods. Analogs of mRNA have been used by several groups (reviewed in refs. 8 and 9; see also refs. 27–29) to affinity label those ribosomal components near to the decoding site. With one exception (30), ribosomal proteins identified as S1, S3, S4, S5, S12, S18, and S21 were found. These protein markers for the mRNA binding region were localized by immuno-EM (1, 31, 32) to the upper one-third region of the particle (illustrated in refs. 16 and 33) in agreement with our results. The correspondence is particularly close in the case of the Lake model (31, 32) in which the protein markers were all found on or near the "platform," corresponding to area 1 in Fig. 5. Since a base in the 3′ one-third of the 16S RNA links the tRNA to the 30S subunit (16), our EM results also serve to localize this region of the 16S RNA on the 30S particle. This, too, is in agreement with other indirect results that have placed proteins associated with this region in the vicinity of mRNA marker proteins (reviewed in refs. 16 and 33), and with direct immuno-EM localization of the 3′-terminal region of 16S RNA (20). Our results also agree with the position of the decoding site proposed in a recent detailed model for the tRNA–ribosome complex (34), although the resolution we have achieved so far is not sufficient to delineate the decoding site so precisely. Antigenic determinants closer to the actual site of crosslinking should help to achieve this objective.

In general, combination of the techniques of affinity labeling with immuno-EM has advantages over either method alone. On the one hand, components that are so weakly bound that they would dissociate under the conditions needed for EM can be specifically fixed to their functional site by crosslinking. On the other hand, placing a hapten on a component that is able to affinity label the ribosome adds the extra dimension of visualization to the topographical results usually obtained from such experiments. The present work is an example of the latter approach.

The authors gratefully acknowledge Miss W. Hellmann and Mr. F. Jenkins for excellent technical assistance.

1. Stöffler, G. & Wittmann, H. G. (1977) in *Molecular Mechanisms of Protein Biosynthesis*, eds. Weissbach, H. & Pestka, S. (Academic, New York), pp. 117–202.
2. Brimacombe, R., Nierhaus, K. H., Garrett, R. A. & Wittmann, H. G. (1976) *Prog. Nucleic Acid Res. Mol. Biol.* **18**, 1–44.
3. Pongs, O., Nierhaus, K. H., Erdmann, V. A. & Wittmann, H. G. (1974) *FEBS Lett.* **40**, S28–S37.
4. Fanning, T. G., Cantrell, M., Shih, C.-Y. T. & Craven, G. R. (1978) *Nucleic Acids Res.* **5**, 933–950.
5. Shimizu, M. & Craven, G. R. (1976) *Eur. J. Biochem.* **61**, 307–315.
6. Thomas, G., Sweeney, R., Chang, C. & Noller, H. F. (1975) *J. Mol. Biol.* **95**, 91–102.
7. Ginzburg, I., Miskin, R. & Zamir, A. (1973) *J. Mol. Biol.* **79**, 481–494.
8. Cooperman, B. S. (1978) in *Bioorganic Chemistry*, ed. van Tamelen, E. (Academic, New York), Vol. 4, pp. 81–115.
9. Zamir, A. (1977) *Methods Enzymol.* **46**, 621–637.
10. Pellegrini, M. & Cantor, C. (1977) in *Molecular Mechanisms of Protein Biosynthesis*, eds. Weissbach, H. & Pestka, S. (Academic, New York), pp. 203–244.
11. Schwartz, I. & Ofengand, J. (1974) *Proc. Natl. Acad. Sci. USA* **71**, 3951–3955.
12. Schwartz, I., Gordon, E. & Ofengand, J. (1975) *Biochemistry* **14**, 2907–2914.
13. Schwartz, I. & Ofengand, J. (1978) *Biochemistry* **17**, 2524–2530.
14. Ofengand, J., Schwartz, I., Chinali, G., Hixson, S. S. & Hixson, S. H. (1977) *Methods Enzymol.* **46**, 683–702.
15. Ofengand, J., Liou, R., Kohut, J., Schwartz, I. & Zimmermann, R. A. (1979) *Biochemistry* **18**, in press.
16. Zimmermann, R. A., Gates, S. M., Schwartz, I. & Ofengand, J. (1979) *Biochemistry* **18**, in press.
17. Schofield, P. & Zamecnik, P. C. (1968) *Biochim. Biophys. Acta* **155**, 410–416.
18. Noll, M., Hapke, B., Schreir, M. H. & Noll, H. (1973) *J. Mol. Biol.* **75**, 281–294.
19. Humayun, M. Z. & Jacob, T. M. (1973) *Biochim. Biophys. Acta* **331**, 41–53.
20. Politz, S. M. & Glitz, D. G. (1977) *Proc. Natl. Acad. Sci. USA* **74**, 1468–1472.
21. Boublik, M., Hellmann, W. & Kleinschmidt, A. K. (1977) *Cytobiologie* **14**, 293–300.
22. Tischendorf, G. W., Zeichhardt, H. & Stöffler, G. (1974) *Mol. Gen. Genet.* **134**, 209–223.
23. Lake, J. A., Pendergast, M., Kahan, L. & Nomura, M. (1974) *Proc. Natl. Acad. Sci. USA* **71**, 4688–4692.
24. Boublik, M. & Hellmann, W. (1978) *Proc. Natl. Acad. Sci. USA* **75**, 2829–2833.
25. Kim, S.-H. (1976) *Prog. Nucleic Acid Res. Mol. Biol.* **17**, 181–216.
26. Willan, K. J., Marsh, D., Sunderland, C. A., Sutton, B. J., Wain-Hobson, S., Dwek, R. A. & Giral, D. (1977) *Biochem. J.* **165**, 199–206.
27. Margaritella, P. & Kuechler, E. (1978) *FEBS Lett.* **88**, 131–134.
28. Fiser, I., Scheit, K. H. & Kuechler, E. (1977) *Eur. J. Biochem.* **74**, 447–456.
29. Towbin, H. & Elson, D. (1978) *Nucleic Acids Res.* **5**, 3389–3407.
30. Wagner, R., Gassen, H. G., Ehresmann, C., Stiegler, P. & Ebel, J.-P. (1976) *FEBS Lett.* **67**, 312–315.
31. Lake, J. A. (1978) in *Advanced Techniques in Biological Electron Microscopy*, ed. Koehler, J. K. (Springer, Berlin), Vol. 2, pp. 173–211.
32. Winkelmann, D. & Kahan, L. (1978) *Fed. Proc. Fed. Am. Soc. Exp. Biol.* **37**, 1739.
33. Kuschler, E. & Ofengand, J. (1979) in *tRNA*, eds. Abelson, J., Schimmel, P. & Söll, D. (Cold Spring Harbor Laboratory, Cold Spring Harbor, NY), in press.
34. Lake, J. A. (1977) *Proc. Natl. Acad. Sci. USA* **74**, 1903–1907.